Neurobiology of Disease

Accumulation of Abnormal Adult-Generated Hippocampal Granule Cells Predicts Seizure Frequency and Severity

Michael S. Hester[1,2] **and Steve C. Danzer**[1,2,3]

[1]Department of Anesthesia and [2]Molecular and Developmental Biology Graduate Program, Cincinnati Children's Hospital Medical Center, Cincinnati, Ohio 45229, and [3]Departments of Anesthesia and Pediatrics, University of Cincinnati, Cincinnati, Ohio 45267

Accumulation of abnormally integrated, adult-born, hippocampal dentate granule cells (DGCs) is hypothesized to contribute to the development of temporal lobe epilepsy (TLE). DGCs have long been implicated in TLE, because they regulate excitatory signaling through the hippocampus and exhibit neuroplastic changes during epileptogenesis. Furthermore, DGCs are unusual in that they are continually generated throughout life, with aberrant integration of new cells underlying the majority of restructuring in the dentate during epileptogenesis. Although it is known that these abnormal networks promote abnormal neuronal firing and hyperexcitability, it has yet to be established whether they directly contribute to seizure generation. If abnormal DGCs do contribute, a reasonable prediction would be that the severity of epilepsy will be correlated with the number or load of abnormal DGCs. To test this prediction, we used a conditional, inducible transgenic mouse model to fate map adult-generated DGCs. Mossy cell loss, also implicated in epileptogenesis, was assessed as well. Transgenic mice rendered epileptic using the pilocarpine-status epilepticus model of epilepsy were monitored continuously by video/EEG for 4 weeks to determine seizure frequency and severity. Positive correlations were found between seizure frequency and (1) the percentage of hilar ectopic DGCs, (2) the amount of mossy fiber sprouting, and (3) the extent of mossy cell death. In addition, mossy fiber sprouting and mossy cell death were correlated with seizure severity. These studies provide correlative evidence in support of the hypothesis that abnormal DGCs contribute to the development of TLE and also support a role for mossy cell loss.

Introduction

Morphologically abnormal dentate granule cells (DGCs) are a prominent feature of temporal lobe epilepsy (TLE) models. Mossy fiber sprouting (MFS) occurs when DGC axons, termed "mossy fibers," project into the dentate inner molecular layer (IML) and form excitatory connections with the proximal apical dendrites of neighboring DGCs (Tauck and Nadler, 1985; Nadler, 2003). MFS has been described in almost all animal models of TLE and has been consistently identified in humans with the condition (Sutula and Dudek, 2007; de Lanerolle et al., 2012). More recently, DGCs with basal dendrites projecting into the dentate hilus have been observed in numerous rodent TLE models (Spigelman et al., 1998; Ribak et al., 2000; Murphy et al., 2012; Sanchez et al., 2012). In rodents, DGCs normally lack basal dendrites, and by projecting into the dentate hilus, these basal processes become targets for mossy fiber innervation. Finally, DGCs with their somata ectopically located in the dentate hilus have been identified in both animals (Scharfman et al., 2000) and humans (Parent et al., 2006) with TLE. These ectopic cells are hypothesized to drive seizures (Scharfman et al., 2000; Cameron et al., 2011).

Unlike many neurons, DGCs are generated throughout life, and, in recent years, it has become clear that the majority of abnormal cells in epilepsy models are newly generated. Both cells <5 weeks old at the time of an insult and cells born after an insult are most vulnerable (Jessberger et al., 2007; Walter et al., 2007; Kuruba et al., 2009; Kron et al., 2010; Murphy et al., 2011; Santos et al., 2011). Abnormal DGCs mediate the formation of recurrent excitatory connections within the dentate (Danzer, 2012), and computational modeling studies support a pro-epileptogenic role for these neurons (Morgan and Soltesz, 2008). Moreover, investigators have found that blocking neurogenesis after an epileptogenic brain injury, thereby reducing the "load" of abnormal newborn cells, reduces the frequency of spontaneous seizures (Jung et al., 2004, 2006). Conversely, increasing the load of abnormal DGCs by deleting the mTOR (mammalian target of rapamycin) pathway inhibitor PTEN (phosphatase and tensin homolog)—which induces abnormal DGC integration—leads to the development of epilepsy in otherwise normal rodents (Pun et al., 2012).

If abnormal integration of newborn DGCs plays a critical role in epileptogenesis, then it would be logical for an animal harboring a greater number of these cells to exhibit a more severe phenotype. Here, we tested this hypothesis by determining whether the percentage of newborn DGCs that integrated abnormally was correlated with seizure frequency or duration. Newborn DGCs were labeled using bitransgenic Gli1–CreER^{T2}::GFP reporter

Received Nov. 1, 2012; revised March 25, 2013; accepted March 26, 2013.

Author contributions: M.S.H. and S.C.D. designed research; M.S.H. and S.C.D. performed research; M.S.H. and S.C.D. contributed unpublished reagents/analytic tools; M.S.H. and S.C.D. analyzed data; M.S.H. and S.C.D. wrote the paper.

This work was supported by National Institute of Neurological Disorders and Stroke Grants R01NS065020 and R01NS062806 (S.C.D.). We thank Raymund Pun for his guidance with electrophysiological techniques, and Keri Kaeding for useful comments on previous versions of this manuscript.

The authors declare no competing financial interests

Correspondence should be addressed to Dr. Steve C. Danzer, 3333 Burnet Avenue, ML 2001, Cincinnati, OH 45229-3039. E-mail: steve.danzer@cchmc.org.

DOI:10.1523/JNEUROSCI.5161-12.2013

 0270-6474/13/338926-11$15.00/0

mice. Seizure frequency and severity were determined by continuous video/EEG monitoring. Although not directly related to neurogenesis, death of hilar mossy cells was also assessed because loss of these neurons is implicated in TLE (Jiao and Nadler, 2007).

Materials and Methods

Animals. All procedures involving animals were approved by the Institutional Animal Care and Use Committee of the Cincinnati Children's Hospital Research Foundation and conform to National Institutes of Health guidelines for the care and use of animals. To generate animals for the present study, hemizygous Gli1–CreER^{T2} mice (Ahn and Joyner, 2004, 2005) were crossed to mice homozygous for a CAG–CAT–EGFP (GFP) reporter construct driven by the CMV-B actin promoter (Nakamura et al., 2006). Nine Gli1–CreER^{T2}::GFP reporter bitransgenic offspring from this cross were used for experiments. All animals were on a C57BL/6 background.

The Gli1 promoter drives CreER^{T2} expression among progenitor cells in the hippocampal subgranular zone. Postnatal tamoxifen treatment of bitransgenic mice activates cre recombinase in these DGC progenitors (Ahn and Joyner, 2005; Murphy et al., 2011), leading to the persistent expression of GFP in the progenitor cells and all of their progeny. Mice were given injections of tamoxifen (250 mg/kg, s.c.) at 3, 5, 7, 9, and 11 weeks of age. At 8 weeks of age, mice received methyl scopolamine nitrate in sterile saline (1 mg/kg, s.c.), followed by pilocarpine (420 mg/kg, s.c.) 15 min later. Animals were monitored behaviorally for seizures and the onset of status epilepticus (SE) (defined as continuous tonic–clonic seizures). After 3 h of SE, mice were given two injections of diazepam 10 min apart (10 mg/kg, s.c.) to mitigate seizure activity. Mice were given sterile Ringer's solution as needed to maintain pretreatment body weight and housed in an incubator overnight at 32°C. Animals were then returned to their home cages, in which they were provided with food and water *ad libitum* with a 14/10 h light/dark cycle.

Although non-epileptic animals (no pilocarpine treatment) were not explicitly included in the present study, we have examined GFP-expressing DGCs in >100 non-epileptic Gli1–CreER^{T2}::GFP mice with tamoxifen injection protocols ranging from P7 to adulthood and survival periods from 1 week to 8 months (Murphy et al., 2011; Pun et al., 2012; our unpublished observations). In all of these animals, we have consistently observed an absence of MFS and incidences of GFP-expressing DGCs with basal dendrites or ectopic somata of ~1% or less. This low rate of DGC abnormalities in controls is consistent with the published literature (Buckmaster and Dudek, 1999; Ribak et al., 2000; Scharfman et al., 2000; McCloskey et al., 2006; Jessberger et al., 2007; Jiao and Nadler, 2007; Walter et al., 2007; Buckmaster, 2012), and because the primary comparison in the present study is among epileptic animals with differing seizure frequencies, additional non-epileptic mice were not included.

Video/EEG monitoring. Tamoxifen-treated Gli1–CreER^{T2}::GFP mice that developed SE ($n = 9$; five males, four females) were implanted with EEG electrodes at 18 weeks of age in accord with established protocols (Castro et al., 2012). Briefly, animals were anesthetized with isoflurane (induction at 3.5%, maintenance at 1.5%), the skull was exposed, and 1-mm-diameter holes were drilled at positions 1.5 mm anterior to lambda and 1.5 mm lateral to midline over each hemisphere. The dura was left intact. A single wire electrode was then positioned in each hole just above the dura. Additional support was provided by setting two skull screws, and the entire assembly was secured with dental cement. Electrode wires fed into a two-lead wireless transmitter (TA11ETA-F10; Data Sciences International), which was placed subcutaneously under the back of each animal. Animals were allowed to recover for 1 week and then housed in 12 × 6.5 × 5.5 inch cages placed on top of the wireless EEG receiver plates (RPC1; Data Sciences International). Animal behavior was monitored by video (resolution, 640 × 480 pixels; Axis 221; Axis Communications). Synchronized video/EEG data was collected continuously for the next 3–4 weeks. Seizures were identified by an investigator blinded to morphological phenotype using Neuroscore software (version 3.4.2; Data Sciences International). Seizures were defined by an initial increase in EEG amplitude (minimum of twice baseline) and progressive frequency changes over the course of the event (typically high-frequency tonic firing followed by clonic bursting and ending with the appearance of theta activity; Fig. 1*A*). To be scored as a seizure, the event had to have a minimum duration of 10 s. Video data were also used to assess the behavioral manifestations of each EEG seizure according to the scale developed by Racine (1972). However, because of the more limited resolution of the video and sometimes poor viewing angle, behavioral stage 1 (mouth and facial movements) and stage 2 (head nodding) seizures were both scored as stage 1.5. At 23 weeks of age, mice were anesthetized with pentobarbital (100 mg/kg, i.p.) and perfused with 1 U/ml heparin, 2.5% paraformaldehyde, and 4% sucrose in PBS, pH 7.4. Brains were removed, postfixed overnight in the same fixative, cryoprotected in ascending sucrose series (10, 20, and 30%) in PBS, and snap frozen in isopentane at −25°C. Brains were sectioned coronally at 60 μm, and sections were mounted to gelatin-coated slides and stored at −80°C.

Immunohistochemistry. Slide-mounted brain sections (two to four per slide) from both dorsal and ventral hippocampus were processed for histological studies. Sections were double immunostained with chicken anti-GFP (1:500; Abcam) and rabbit anti-zinc transporter 3 (ZnT3) (1:3000; Synaptic Systems), rabbit anti-glutamate receptor 2 (GluR2) (1:200; Millipore), or mouse anti-calretinin (1:1000; Millipore). Alexa Fluor 488 goat anti-chicken, Alexa Fluor 594 goat anti-rabbit, and Alexa Fluor 594 goat anti-mouse secondary antibodies were used (Invitrogen). Tissue was dehydrated in alcohol series and cleared in xylenes, and coverslips were secured with mounting media (Krystalon; Harleco).

Confocal microscopy and histological analyses. Imaging was conducted using a Leica SP5 confocal system set up on a DMI 6000 inverted microscope equipped with a 63× oil-immersion objective (numerical aperture 1.4). Images were collected by an investigator blind to seizure score. For each parameter, dentate gyri were analyzed from the left and right hemispheres for dorsal (2 mm posterior to bregma) and ventral (3 mm posterior to bregma; Paxinos and Franklin, 2001) hippocampus (four dentate gyri per animal).

To assess basal dendrite frequency, images of GFP-expressing cells were collected at 0.5 μm increments through the 60 μm *z*-depth of the tissue section to generate three-dimensional confocal *z*-stacks. For dorsal hippocampus, two complete dentate gyri per animal were imaged. For ventral hippocampus, a similar strategy was used; however, because of the larger size, left and right dentate gyri were sampled. Specifically, confocal image stacks through the *z*-depth were collected from the midpoint of both the upper and lower blades of the dentate cell body layer (four confocal *z*-stacks each with a field size 240 × 240 μm). Image stacks were imported into Neurolucida software to determine the percentage of GFP-expressing DGCs that also possessed basal dendrites projecting into the dentate hilus. Basal dendrites were distinguished from axons by their greater diameter and presence of dendritic spines. Basal dendrites were only counted for mature DGCs if their cell bodies were fully contained within the tissue section and correctly located in the DGC layer (normotopic DGCs). Mature DGCs were distinguished by the presence of a spiny apical dendrite projecting through the molecular layer and terminating at the hippocampal fissure and a basal axon extending into the hilus. Only DGCs with robust GFP labeling, such that dendritic structures were clearly revealed, were analyzed. All DGCs meeting selection criteria were scored.

To determine the percentage of newborn DGCs that were ectopic, dentate gyri were screened under epifluorescent illumination. DGCs were scored as ectopic if their cell body was located in the hilus and was at least two cell body diameters (~20 μm) from the DGC layer–hilar border. Ectopic cells were counted using a variation of the optical dissector method (Howell et al., 2002).

To assess DGC mossy fiber axon sprouting, confocal optical sections of ZnT3 labeling were collected from the midpoint of the upper and lower blades of the dentate gyrus. Images were collected using identical confocal settings for each animal (63×; excitation wavelength, 543 nm; 100% power; emission range collected, 500–550 nm). To control for antibody penetration gradients, confocal optical sections were collected 3 μm below the surface of the tissue section for all samples. The area of ZnT3-immunoreactive puncta within the dentate IML was quantified using Neurolucida software (version 3.4.2). Puncta were defined as ZnT3-

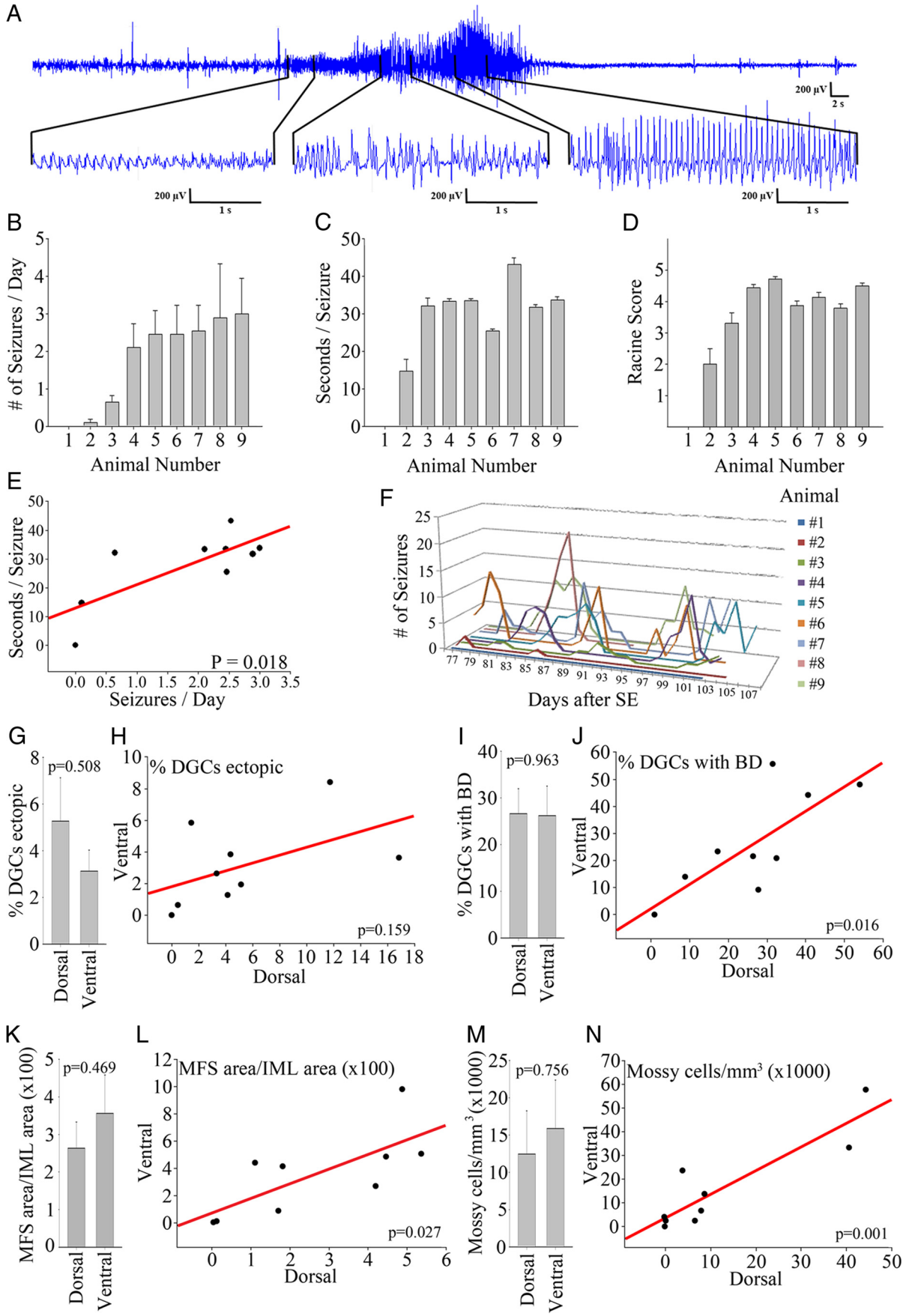

Figure 1. EEG and hippocampal abnormalities in pilocarpine-treated animals. Cortical EEG recording showing a spontaneous seizure (***A***). Seizure frequencies in animals exhibiting pilocarpine-induced SE ranged from zero to three seizures per day (***B***). The average spontaneous seizure duration between animals ranged from 15 to 43 s per seizure (***C***), with (*Figure legend continues.*)

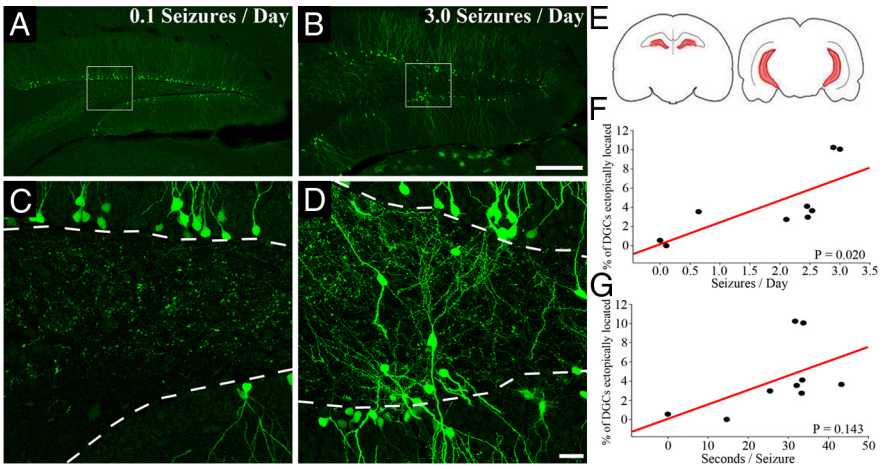

Figure 2. Ectopically located newborn granule cells correlate with seizure frequency. Images are confocal maximum projections showing GFP-expressing newborn granule cells in the dorsal hippocampus of bitransgenic mice. Mice experienced 0.1 (***A***, ***C***) and 3.0 (***B***, ***D***) seizures per day. ***C*** and ***D*** are higher-resolution images of the boxed regions in ***A*** and ***B***, respectively. The dentate hilus in each image is located between the dotted lines. Note the large number of ectopic granule cells in ***D*** and the absence of such cells in ***C***. ***E***, Schematics showing the sample regions in red for ectopic cell measures for dorsal and ventral hippocampus (the entire hilus). ***F***, ***G***, The percentage of newborn granule cells ectopically located in the dentate hilus was significantly correlated with seizure frequency but not seizure duration (regression line is in red). Scale bars: ***A***, ***B***, 250 μm; ***C***, ***D***, 20 μm.

Table 1. Pearson's product moment correlations (*R*) and *p* values for each morphological parameter versus seizure frequency, seizure duration, and Racine score in dorsal (D) and ventral (V) hippocampus and both combined (D + V)

	D + V (*R*)	D + V (*p*)	D (*R*)	D (*p*)	V (*R*)	V (*p*)
% DGCs ectopic						
Frequency	0.751	0.020*	0.619	0.076	0.763	0.017*
Duration	0.529	0.143	0.386	0.305	0.641	0.063
Racine	0.467	0.243	0.324	0.434	0.583	0.129
% DGCs with basal dendrites						
Frequency	0.489	0.182	0.617	0.077	0.326	0.392
Duration	0.657	0.054	0.763	0.017*	0.494	0.176
Racine	0.562	0.147	0.595	0.120	0.448	0.265
% IML with MFS						
Frequency	0.673	0.047*	0.774	0.014*	0.527	0.145
Duration	0.713	0.031*	0.746	0.021*	0.609	0.082
Racine	0.806	0.016*	0.846	0.008*	0.664	0.072
Mossy cell density						
Frequency	−0.793	0.011*	−0.857	0.003*	−0.695	0.038*
Duration	−0.845	0.004*	−0.879	0.002*	−0.773	0.015*
Racine	−0.922	0.001*	−0.932	0.001*	−0.81	0.015*

*$p < 0.05$.

immunoreactive regions with a diameter >0.5 μm. The degree of MFS was defined as [(MFS area/total IML area) × 100].

The density of mossy cells in the hilus was determined from confocal image stacks of GluR2 labeling. Images stacks were captured from a 240 × 240 μm scanning field placed in the center of the hilus. Image stacks were collected with a 0.5 μm step through 10 μm of tissue, beginning 3 μm below the surface to avoid regions damaged by cryosectioning. The hilar area in each image stack was calculated using Neurolucida software by drawing a contour around the hilar border. Sample volume was determined by multiplying the hilar area examined by the depth of tissue imaged (10 μm). GluR2-positive mossy cells were counted using a variation of the optical dissector method (Howell et al., 2002). Small hilar GluR2-immunoreactive cells (8–12 μm diameter) were considered to be ectopic DGCs and were excluded, whereas larger GluR2-expressing neurons (30–40 μm diameter) localized to the hilus were counted as mossy cells (Fujise and Kosaka, 1999; Jiao and Nadler, 2007; Scharfman and Myers, 2012). Mossy cell hilar density is presented as GluR2-expressing hilar mossy cells per cubic millimeter of hilus. For comparative purposes, mossy cell density was also determined in five C57BL/6 control (non-epileptic) mice.

Statistics. Statistical analyses were performed using SigmaStat software (version 12.3). Seizure frequency, seizure duration, Racine score, and the number and percentages of abnormal cells were similar between males and females (data not shown), so data were pooled for analysis. In the interest of thoroughness, correlations were generated using several different approaches. First, correlations were generated for dorsal and ventral hippocampus separately and then for dorsal and ventral regions combined. In the first case, the possibility that one region might predominate was explored, and in the second, the goal was to examine the impact of the overall load of abnormal cells throughout the hippocampus. Data were combined by taking the average of dorsal and ventral measures for each animal. In addition, correlations were generated using normalized data, in which the percentage of newborn DGCs that integrated abnormally was determined using the following equations: for ectopic cells, ectopic GFP-expressing DGCs per dentate per total GFP-expressing DGCs per dentate; and for cells with basal dendrites, normatopic GFP-expressing mature DGCs with basal dendrites per dentate per total normatopic GFP-expressing mature DGCs per dentate. Because the efficiency of tamoxifen-induced recombination is not 100% (not all newborn cells are labeled), data were normalized to the number of GFP-expressing cells to ensure that artifactual changes in tamoxifen-induced recombination efficiency did not impact the results (i.e., differences in tamoxifen absorption/distribution attributable to animal adipose tissue content or health; Lien et al., 1991). Parametric tests were used for data that met assumptions of normality and equal variance, whereas nonparametric versions of these tests were used for data that violated one or both assumptions. Pearson's product moment correlation was used unless otherwise specified in the text. p values < 0.05 were considered significant. Values are presented as means ± SEM.

Figure preparation. Figures were prepared using Adobe Photoshop (CS5-Extended; Adobe Systems). Brightness and contrast were adjusted to optimize cellular detail. Identical adjustments were made to all images meant for comparison.

Results

Seizure frequency and duration after pilocarpine-induced SE

To determine seizure frequency among pilocarpine-treated mice, continuous video/EEG data were recorded from neocortex for 3–4 weeks, beginning 11 weeks after SE. Eight of the nine pilocarpine-treated mice exhibited spontaneous recurrent seizures during the recording period (Fig. 1*A*,*B*,*F*). Whether the one animal that exhibited no seizures would have developed epilepsy at later time points is not known. In addition, because EEG measures are limited to the brain regions in proximity to the electrodes (neocortex), the possibility that seizures occurring in

←

(*Figure legend continued.*) higher seizure frequencies being positively correlated with longer seizure durations (***E***). The average behavioral seizure score for each animal ranged from 2.0 to 4.4 (***D***). Four weeks of 24 h video/EEG monitoring revealed the typical "seizure clustering" phenomenon associated with the pilocarpine model (***F***). No significant differences were found between dorsal and ventral hippocampus for the percentage of ectopic DGCs (***G***), the percentage of DGCs harboring basal dendrites (BD; ***I***), the percentage increase of MFS (***K***), or hilar mossy cell density (***M***). Dorsal and ventral hippocampus were significantly correlated for the percentage of newborn DGCs with basal dendrites (***J***), MFS (***L***), and density of surviving mossy cells (***N***) but not for ectopic DGCs (***H***). Error bars are means ± SEM.

other brain regions were missed cannot be excluded. However, all animals had electrodes placed at the same coordinates, so comparisons among animals are justified.

A total of 423 electrographic seizures were recorded for all animals combined. Seizure frequency among the eight animals with confirmed epilepsy ranged from 0.1 to 3.0 seizures per day (Fig. 1*B*; mean for all animals combined was 1.8 ± 0.4 seizures/d). Seizure duration was variable among animals, averaging from 15 to 43 s per seizure (Fig. 1*C*; mean for all animals combined was 27.5 ± 4.3 s/seizure). For the majority of EEG seizures (414), behavioral changes were observed according to the scale developed by Racine (Racine, 1972). The average Racine score for all animals combined was 3.8 ± 0.3 (the range of individual animal averages was 2.0–4.4; Fig. 1*D*). Racine score was significantly correlated to both seizure frequency ($p = 0.017$, $r = 0.803$) and seizure duration ($p = 0.027$, $r = 0.764$). Similarly, a significant correlation was found between high seizure frequency and longer seizure duration (Fig. 1*E*; $p = 0.018$, $r = 0.760$).

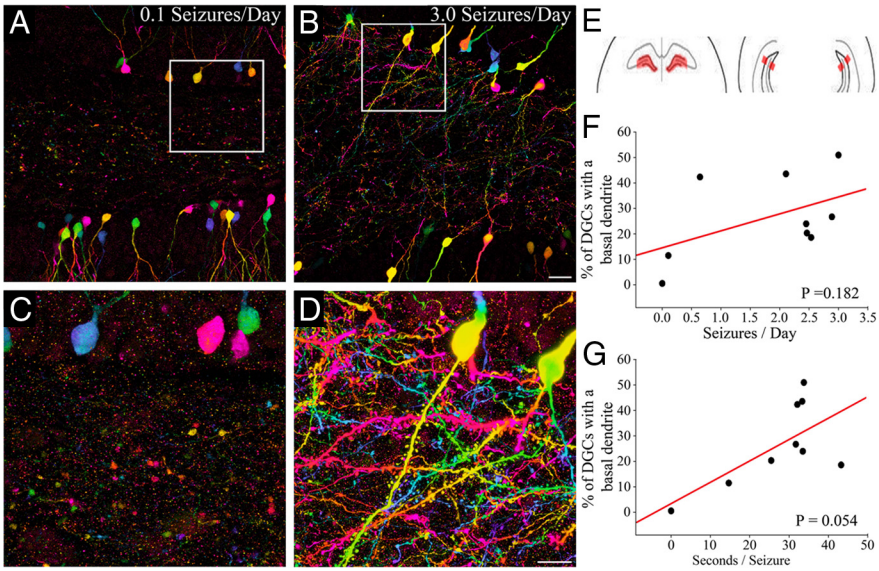

Figure 3. Basal dendrites and seizure frequency. Images are confocal maximum projections from dorsal hippocampus showing GFP-expressing newborn granule cells with (***B***, ***D***) and without (***A***, ***C***) basal dendrites. Images have been processed using a depth filter, which assigns different colors to processes located at different depths within the tissue. Mice had mean seizure frequencies of 0.1 (***A***, ***C***) and 3.0 (***B***, ***D***) seizures/d. ***C*** and ***D*** are high-magnification images of the boxed regions in ***A*** and ***B***, respectively. The entire dentate was scored for dorsal hippocampus (***E***, region in red in the left), whereas ventral hippocampus was sampled in the upper and lower blades of both hemispheres (***E***, right). ***F***, ***G***, Scatter plots display a nonsignificant trend between the percentage of normotopic DGCs harboring basal dendrites and seizure frequency and duration (regression line is in red). Scale bars: ***A***, ***B***, 20 μm; ***C***, ***D***, 10 μm.

There were no overt changes in seizure frequency (Fig. 1*F*) or duration (data not shown) within animals during the recording period. There were also no day/night differences in seizure frequency ($p = 0.597$, *t* test). However, seizures did tend to occur in clusters (Fig. 1*F*), consistent with previous studies (Goffin et al., 2007; Bajorat et al., 2011). Clusters were defined as the occurrence of five or more seizures preceded by and followed by at least 2 or more seizure-free days. Clusters lasted an average of 5.2 ± 0.3 d with a mean of 27.9 ± 3.3 seizures per cluster. The mean seizure-free period between clusters was 6.7 ± 0.8 d. One animal (#8), which exhibited the largest seizure cluster (52 seizures in 5 d), became moribund in the days thereafter and was killed after 3 weeks of monitoring for animal welfare considerations. No other animals displayed declining health during the 4 week recording period.

GFP labeling of newborn DGCs

DGCs arising from recombined progenitor cells displayed robust GFP expression. Fine neuronal structures, such as axons and spines, were clearly distinguishable, providing more than ample resolution for the purposes of this study. For dorsal hippocampus, a total of 1710 GFP-expressing newborn DGCs were scored for both hilar basal dendrites and ectopic somata (range, 30–308 cells per animal; mean, 190 ± 35 cells per animal). For ventral hippocampus, all GFP-expressing DGCs present in the section were counted to determine the percentage of ectopic cells, as for dorsal hippocampus, yielding a total of 2718 DGCs (range, 119–575 cells per animal; mean, 302 ± 53 cells per animal). However, because of the larger size of ventral hippocampus, GFP-expressing cells were sampled to determine the percentage with basal dendrites (see Materials and Methods). A total of 330 normotopic DGCs from ventral hippocampus were scored for hilar basal dendrites (range, 18–53 cells per animal; mean, 37 ± 4 cells per animal).

Sections from a subset of animals ($n = 3$) were immunostained with GFP and the immature granule cell marker calretinin to assess recombination efficiency. Three months after the last tamoxifen injection, 5.9 ± 1.5% of immature (calretinin-immunoreactive) DGCs expressed GFP, indicating that the Gli1–CreER^{T2} fate-mapping strategy used for the present study provides a reasonable sample of newborn DGCs throughout the experimental period.

Dorsal versus ventral hippocampus

The dorsal and ventral regions of the hippocampus are morphologically and functionally distinct (Fanselow and Dong, 2010); however, robust DGC neurogenesis occurs in both regions (Kaplan and Hinds, 1977; Jinno, 2011). To determine whether epileptogenesis differentially affects newborn cells generated in dorsal versus ventral hippocampus, measures of abnormal DGC integration were compared across regions and correlated within animals. Overall, there were no differences in dorsal versus ventral means for any parameter for all nine animals combined (Fig. 1*G*,*I*,*K*,*M*). In dorsal hippocampus, 5.3 ± 1.9% of newborn DGCs were ectopically located in the hilus, whereas 3.1 ± 0.9% of ventral cells were ectopic (Fig. 1*G*; $p = 0.508$, Mann–Whitney rank-sum test). In dorsal hippocampus, 26.7 ± 5.4% of newborn normotopic DGCs had basal dendrites, whereas 26.3 ± 6.3% of ventral newborn normotopic DGCs possessed basal dendrites (Fig. 1*I*; $p = 0.963$, *t* test). The degree of MFS was also similar between regions (Fig. 1*K*; dorsal, 2.6 ± 0.1% of IML area occupied by MFS; ventral, 3.6 ± 1.0%; $p = 0.469$, *t* test). Last, the density of surviving hilar mossy cells was similar between regions (Fig. 1*M*; dorsal, 12.5 ± 5.8 cells/mm^3; ventral, 15.9 ± 6.4 cells/mm^3; $p = 0.756$, Mann–Whitney rank-sum test). Within animals, most measures for dorsal and ventral parameters were significantly correlated. This was true for the percentages of newborn cells with basal dendrites (Fig. 1*J*; $r = 0.767$, $p = 0.016$), the amount of MFS (Fig. 1*L*; $r = 0.726$, $p = 0.027$) and density of surviving mossy cells (Fig. 1*N*; $r = 0.897$, $p = 0.001$). The one

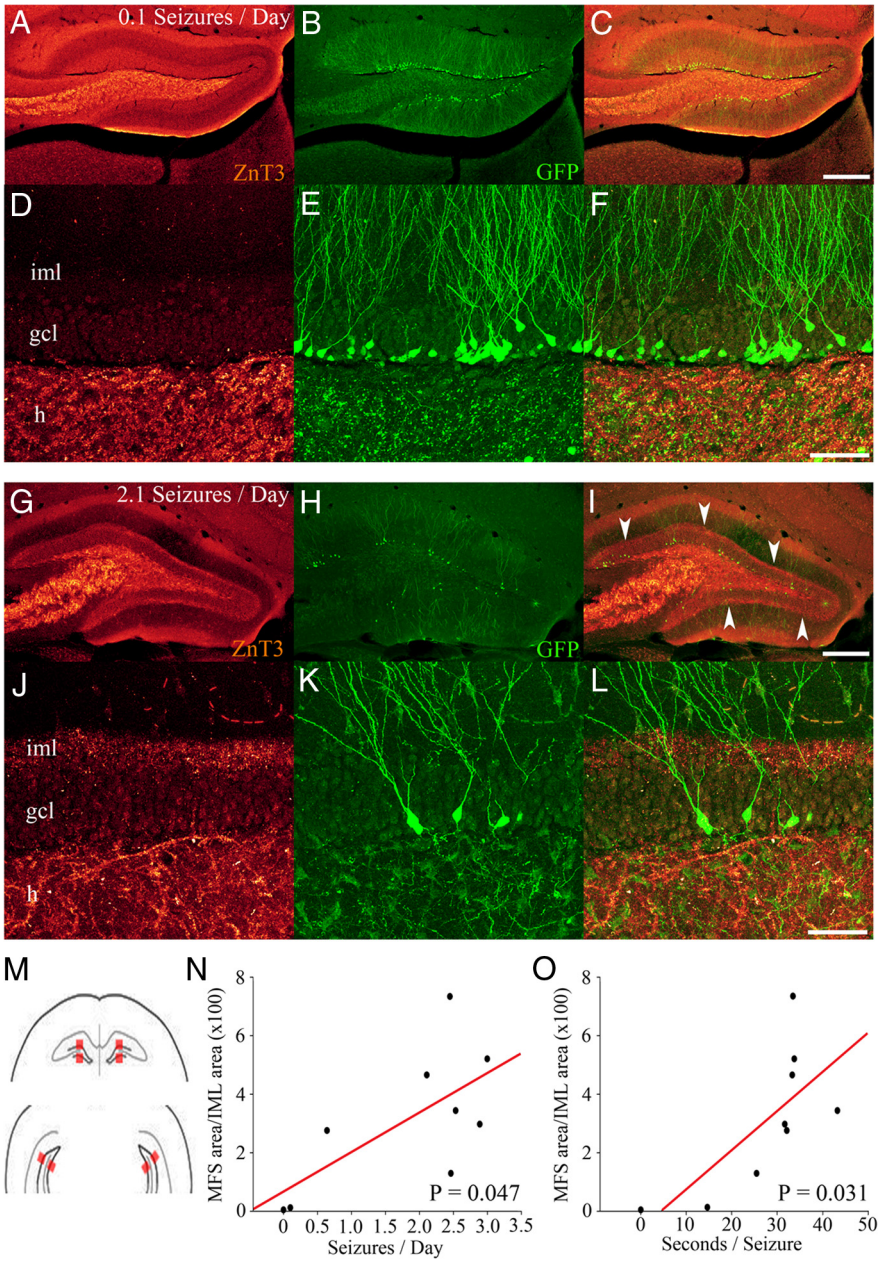

Figure 4. MFS correlates with seizure frequency and duration. Images are confocal maximum projections showing ZnT3 and GFP immunostaining in dorsal hippocampus of mice that exhibited means of 0.1 (***A–F***) and 2.1 (***G–L***) seizures per day. Arrowheads (***I***) highlight sprouted granule cell mossy fiber axons within the dentate IML. ***M***, Schematics showing the sample regions in red for MFS measures for dorsal and ventral hippocampus. Greater MFS density was significantly correlated with increased seizure frequency (***N***) and seizure duration (***O***) (regression line is in red). GCL, Granule cell layer; h, hilus. Scale bars: ***A–C***, ***G–I***, 250 μm; ***D–F***, ***J–L***, 50 μm.

exception was ectopic cells, in which no correlation between regions was found (Fig. 1*H*; $r = 0.512$, $p = 0.159$). Together, these findings suggest that SE and the development of spontaneous seizures have similar impacts on DGC plasticity and mossy cell death in dorsal and ventral regions of the hippocampus. Although measurements were collected from a subset of sections from the two hippocampal regions, the correspondence between these relatively disparate regions suggests that our measures are likely representative of the entire hippocampus.

Ectopic DGCs significantly correlate with seizure frequency but not seizure duration

The percentage of newborn DGCs that were ectopic was significantly correlated with seizure frequency for dorsal and ventral hippocampus combined (Fig. 2*F*, Table 1). Regionally, dorsal hippocampus did not significantly correlate to the percentage of ectopic DGCs, whereas ventral hippocampus did reach significance, although the trend was similar in both regions. The ectopic DGC population constituted <1% of all newborn DGCs in animals exhibiting the fewest seizures (≤0.1 seizures/d); ectopic DGCs were essentially absent from these animals (Fig. 2*A*,*C*). Conversely, animals with the highest seizure frequencies (>2.8 seizures/d) contained ectopic DGC populations exceeding 10% of all newborn DGCs (Fig. 2*B*,*D*). There was no significant correlation between the percentage of hilar ectopic DGCs and seizure duration, for either dorsal and ventral hippocampus combined or individually (Fig. 2*G*, Table 1). There was also no correlation between Racine score and the percentage of hilar ectopic DGCs (Table 1).

The percentage of normotopic DGCs with basal dendrites does not correlate with seizure frequency but may be linked with seizure duration

Basal dendrites were present on a substantial portion of the newborn DGC population (>10%) in all eight animals exhibiting at least one seizure, whereas the single animal with no observed seizures possessed almost no DGCs with basal dendrites (<1%). In the animal exhibiting the greatest frequency of seizures, >50% of the GFP-expressing newborn DGCs possessed basal dendrites (Fig. 3*B*,*D*). Conversely, the animal exhibiting only 0.1 seizures/d was comparatively free of basal dendrites (Fig. 3*A*,*C*). Despite these trends, there was no significant correlation between the percentage of newborn cells with basal dendrites and seizure frequency for dorsal and ventral hippocampus combined (Fig. 3*F*, Table 1). Similarly, neither region produced significant correlations when examined individually. However, there was a significant positive correlation between basal dendrites and seizure duration within dorsal hippocampus. This effect was absent from ventral hippocampus and did not quite reach significance for dorsal and ventral combined (Fig. 3*G*, Table 1). There was no correlation between Racine score and the percentage of normotopic DGCs containing basal dendrites (Table 1).

The intensity of MFS significantly correlates with seizure frequency and seizure duration

Sprouting of DGC mossy fiber axons into the dentate IML was assessed in each animal by ZnT3 immunohistochemistry. ZnT3 labeling reveals the axon terminals of both mature and newborn DGCs and provides a reliable measure of MFS (McAuliffe et al., 2011; Murphy et al., 2011). Mice that had few seizures exhibited

little to no MFS (Fig. 4*A–F*), whereas mice exhibiting high seizure frequencies showed robust MFS in the IML (Fig. 4*G–L*). The degree of MFS was significantly correlated with seizure frequency for dorsal and ventral hippocampus combined, but only dorsal hippocampus reached significance when analyzed separately (Fig. 4*N*, Table 1). Additionally, MFS and seizure duration were significantly correlated when both regions were combined (Fig. 4*O*, Table 1). The correlation was most robust in dorsal hippocampus, whereas only a trend was evident in ventral hippocampus (Table 1). The average Racine score paralleled the correlations between seizure duration and MFS (Table 1).

Mossy cell loss significantly correlates with seizure frequency and seizure duration

Mossy cells are extremely vulnerable to seizure-induced cell death (Sloviter, 1987; Scharfman et al., 2001; Danzer et al., 2010). Because loss of mossy cells has been proposed as a mediator of epileptogenesis (Sloviter et al., 2012), we sought to establish whether the extent of cell loss correlated with seizure frequency. To assess loss of mossy cells from the dentate hilus, sections were immunostained for GluR2. GluR2 is expressed by glutamatergic mossy cells, which project into the dentate IML. Consistent with previous studies, pilocarpine treatment significantly reduced mossy cell density relative to control (non-epileptic) mice (control, $n = 5$, 57.3 ± 4.7; epileptic, $n = 9$, 14.2 ± 6.0; $p = 0.005$, Mann–Whitney rank-sum test). Within pilocarpine-treated animals, we found a significant, negative correlation between the density of GluR2-expressing mossy cells and seizure frequency (Fig. 5*D*, Table 1). Both dorsal and ventral hippocampus reached significance individually. Mice exhibiting the fewest seizures (≤0.1 seizures/d) contained a dense network of mossy cells in the hilar area (Fig. 5*A*), whereas mice with frequent seizures contained few, if any, mossy cells (Fig. 5*B*). Additionally, there was a significant negative correlation between mossy cell density and seizure duration for dorsal and ventral hippocampus combined and individually (Fig. 5*D*, Table 1). The same pattern of correlations was found between Racine score and mossy cell loss (Table 1). Of note, there was also a significant negative correlation between the density of surviving mossy cells and the amount of MFS ($r = -0.743$, $p = 0.022$).

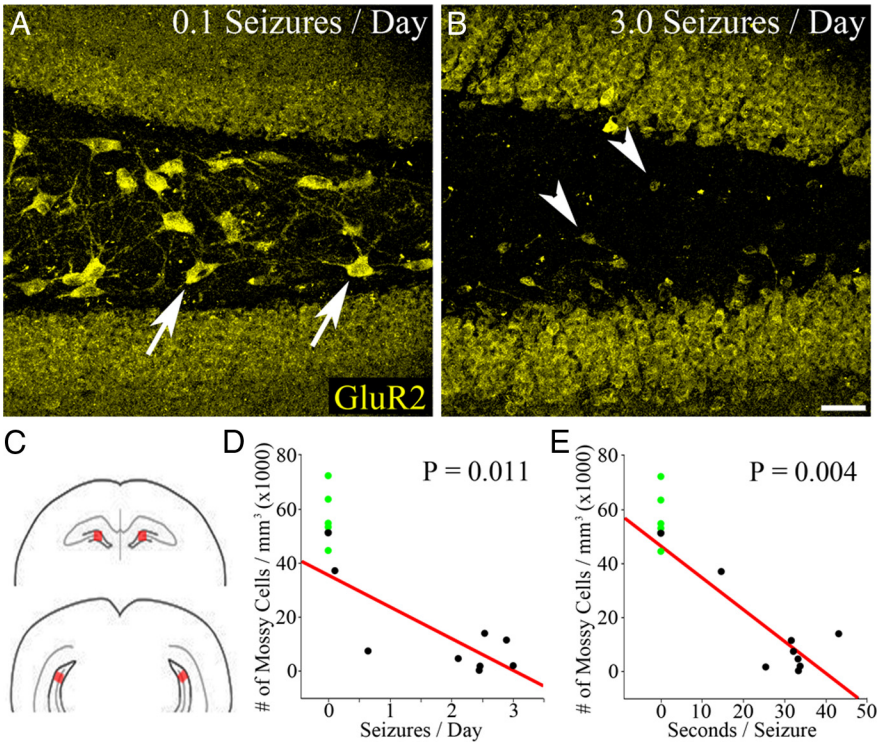

Figure 5. Mossy cells density negatively correlates with seizure frequency and duration. Images are confocal maximum projections of GluR2 immunoreactivity in ventral hippocampus of mice that exhibited means of 0.1 (***A***) and 3.0 (***B***) seizures per day. Arrows denote presumptive mossy cells, whereas arrowheads denote presumptive hilar ectopic granule cells. Note the almost complete loss of mossy cell labeling in ***B***. ***C***, Schematics showing the sample regions in red for mossy cell counts for dorsal and ventral hippocampus. ***D***, ***E***, Scatter plots show low hilar mossy cell density in mice exhibiting high seizure frequency and duration (regression line is in red). Green dots denote mossy cell densities of age-matched control mice that did not undergo SE (not included for statistical analysis of correlations). Scale bar, 25 μm.

Seizure frequency is not correlated with the number of GFP-expressing neurons or the percentage of newborn cells that developed as astrocytes

The total number of GFP-expressing DGCs/hippocampal section was not significantly correlated with either seizure frequency or duration. This was true for both dorsal and ventral hippocampus (dorsal, seizure frequency, $r = -0.058$, $p = 0.882$; seizure duration, $r = -0.144$, $p = 0.711$; ventral, seizure frequency, $r = 0.309$, $p = 0.419$; seizure duration, $r = 0.061$, $p = 0.877$). Finally, although the overwhelming majority of GFP-expressing cells within the hippocampal dentate gyrus of epileptic Gli1–CreER^{T2} mice were DGCs ($96.3 \pm 1.1\%$), a small number of cells meeting morphological criteria for protoplasmic astrocytes were found. GFP-expressing astrocytes ranged from 2 to 17 per hippocampal section. Their percentage as total number of GFP-positive cells did not significantly correlate with seizure frequency ($p = 0.083$, $r = 0.607$), duration ($p = 0.322$, $r = 0.373$), or racine score ($p = 0.101$, $r = 0.620$).

Examination of all four variables combined predicts seizure frequency best

Among the nine animals examined, there were three clear jumps in seizure frequency (Table 2; group 1, 0.0–0.1 seizures/d; group 2, 0.1–0.64; group 3, 0.64 to >2.0). We took advantage of these jumps to query whether there were any notable changes in pathology within each group between the low and high seizure animals. This exercise produced two observations. First, no single pathology consistently increased in severity in the high seizure animals relative to the low. Indeed, some measures of pathology actually improved with greater seizure frequency in individual animals (e.g., basal dendrites for animals 6 and 7 vs animal 3; up arrows). Second, however, in all but one case (animals 7 vs 3), at least one of the four variables did increase in severity (change of 50% or more; Table 2, down arrows). To quantify this effect, the animals were ranked from one to nine in order of increasing severity for each parameter, and the four rank values were added to generate a single "DGC abnormality measure" for each animal. Statistical analysis of this combined measure found that it significantly correlated with seizure frequency ($r = 0.816$, $p = 0.007$).

Table 2. Raw data ranked by increasing seizure frequency

	Animal #	Seizure Duration	Seizure Frequency	% DGCs Ectopic	% DGCs with BDs	% IML with MFS	Mossy Cells / mm^3 (x1000)
Group 1	1	0.00	0.00	0.55	0.47	0.04	51.11
	2	14.67	0.10	▲ 0.00	▼ 11.43	▼ 0.12	37.00
Group 2	2	14.67	0.10	0.00	11.43	0.12	37.00
	3	32.11	0.64	▼ 3.54	▼ 42.33	▼ 2.76	▼ 7.23
Group 3	3	32.11	0.64	3.54	42.33	2.76	7.23
	4	33.36	2.11	2.73	43.54	▼ 4.66	4.42
	5	33.49	2.45	4.11	23.92	▼ 7.35	▼ 0.00
	6	25.46	2.46	2.97	▲ 20.29	▲ 1.29	▼ 1.30
	7	43.24	2.54	3.65	▲ 18.55	3.44	▲ 13.71
	8	31.71	2.89	▼ 10.24	26.65	2.98	▲ 11.13
	9	33.77	3.00	▼ 10.06	50.95	▼ 5.21	▼ 1.83

Three groups are presented comparing animals with large differences in seizure frequency [group 1, animal 2 vs 1 (0.1 vs 0 seizures/d); group 2, animal 3 vs 2 (0.64 vs 0.1 seizures/d); group 3, animals 4–9 vs 3 (>2 vs 0.64 seizures/d)]. Up arrows denote parameters that improved with increasing seizure frequency (50% decrease in severity or more), and down arrows denote parameters that became more severe with increasing seizure frequency (50% increase in severity or more). BD, Basal dendrites.

These findings suggest that examination of all four variables together may better account for the differences in seizure frequency among animals than examination of any single variable alone.

Discussion

Abnormal integration of adult-generated DGCs has been hypothesized to promote the development of TLE (Parent and Lowenstein, 2002). If abnormal DGCs promote epileptogenesis, then animals with a greater number or load of abnormal cells could be predicted to exhibit more frequent seizures. To test this hypothesis, we conducted continuous video/EEG monitoring studies in epileptic mice in which newborn DGCs were labeled with GFP using a genetic fate-mapping approach. The present study revealed a significant positive correlation between aberrantly integrated newborn DGCs and seizure frequency; specifically, animals possessing a substantial percentage of ectopic newborn DGCs and robust MFS exhibited seizures more often than epileptic animals in which a smaller percentage of newborn cells developed abnormally. Although correlative, these findings are consistent with the hypothesis that abnormal DGCs promote temporal lobe epileptogenesis. In addition to the positive correlations between abnormal newborn DGCs and seizure frequency, a negative correlation was found between seizure frequency and the density of remaining hilar mossy cells, such that animals with the lowest density of surviving cells experienced seizures at the highest rate. Therefore, in addition to a role for newborn DGCs, the present findings support a role for mossy cell death in epileptogenesis. Finally, robust MFS and extensive mossy cell death were both significantly correlated with seizure duration and behavioral seizure score. These findings are important because they suggest that—in addition to regulating the incidence of seizures—dentate pathology might also regulate seizure severity. Together, the present findings provide new correlative evidence suggesting that aberrant neuronal integration, potentially acting in concert with cell loss, are key steps in temporal lobe epileptogenesis.

Relationship to previous studies

The present study was designed to assess the key morphological abnormalities found among newborn DGCs in the epileptic brain, as follows: (1) MFS; (2) aberrant basal dendrites; and (3) hilar ectopic DGCs (Parent et al., 2006; Walter et al., 2007; Kron et al., 2010; Murphy et al., 2011). In addition, loss of hilar mossy cells was assessed, because death of these neurons has been proposed as a key step in temporal lobe epileptogenesis (Sloviter et al., 2012). Although correlations between some of these variables and seizures have been examined in previous studies (Mathern et al., 1997; Gorter et al., 2001; McCloskey et al., 2006), to our knowledge, this is the first study to examine all of these changes in the same animals.

Technical aspects of the present study

Examination of numerous parameters was made possible by using Gli1–CreER^{T2}::GFP reporter-expressing bitransgenic mice. Treatment of these animals with tamoxifen leads to cre-mediated recombination and persistent GFP expression in Gli1-expressing DGC progenitors. Gli1 is a transcription factor that is activated by the sonic hedgehog (Shh) signaling pathway. Shh is a critical regulator of adult neurogenesis in the dentate (Lai et al., 2003; Pozniak and Pleasure, 2006; Han et al., 2008), so the Gli1–CreER^{T2} mice are a useful tool for selective labeling of adult-generated cells. Not all granule cell progenitors undergo recombination after tamoxifen treatment in these animals; only 6% of recently generated cells in our study expressed GFP 3 months after the last tamoxifen injection (calretinin-expressing cells are ~2 weeks old). Nonetheless, this is sufficient to provide a sample of the newborn cell population, and the percentage of recombined cells may have been higher at earlier time points. Importantly, studies by Ahn and Joyner (2005) indicate that the recombined cells are representative of the Shh-responding population. Consistent with this interpretation, the types of abnormalities observed in the present study, as well as the proportions of cells showing abnormalities, were similar to previously pub-

lished studies using a variety of different approaches (Buckmaster and Dudek, 1999; Jessberger et al., 2007; Walter et al., 2007; Kron et al., 2010; Murphy et al., 2011; Santos et al., 2011; Ribak et al., 2012). These observations support the conclusion that the bitransgenic labeling strategy used here provides a reliable measure of aberrant DGC integration rates.

The present study also takes advantage of new technologies that greatly simplify continuous seizure monitoring. Monitoring animals continuously can be critical, especially for the pilocarpine model, because seizures can occur in clusters (Goffin et al., 2007; Bajorat et al., 2011; Fig. 1*F*), a phenomenon also seen in epileptic patients (Haut et al., 2002, 2005). Intermittent monitoring that misses even a single seizure cluster could dramatically underestimate seizure frequency, and improved techniques may account for the conflicting findings between the present work and past studies that did not use continuous EEG monitoring (Cronin and Dudek, 1988) or monitored for only brief periods (Pitkanen et al., 2000; Nissinen et al., 2001).

Seizure frequency in the pilocarpine model is unpredictable, and, in the present study, animals tended to exhibit either high or low rates (Fig. 1*B*). We would predict, based on the current findings, that animals with intermediate seizure rates will exhibit intermediate levels of abnormal DGC integration. However, until additional studies can be conducted with more animals representing intermediate seizure frequencies, the present findings should be interpreted with the more limited dataset in mind.

Significance of correlations between dentate pathology and seizure frequency

In different ways, all four pathologies examined here are hypothesized to promote epileptogenesis. First, ectopic migration of DGCs has been observed in numerous rodent models of TLE (Parent et al., 1997; Scharfman et al., 2000; Dashtipour et al., 2001; Bonde et al., 2006; Fournier et al., 2010), as well as in tissue samples from epileptic humans (Parent et al., 2006). These cells receive a disproportionate amount of excitatory input compared with normotopic DGCs. Furthermore, these cells have been shown to generate spontaneous epileptiform bursts (Scharfman et al., 2000; Cameron et al., 2011), a phenomenon that is absent from normotopic DGCs. Therefore, it is conceivable that hilar DGCs act as seizure initiating "hub cells," which have been hypothesized to play a key role in epileptogenesis (Scharfman and Pierce, 2012). Second, MFS has long been associated with the epileptic brain (Tauck and Nadler, 1985). The formation of recurrent excitatory circuits via MFS has made the phenomena an attractive candidate as a key regulator of dentate hyperexcitability (Golarai and Sutula, 1996). Third, DGC basal dendrites, by projecting aberrantly into the dentate hilus, become targets for innervation by DGC mossy fiber axons, which normally form extensive collaterals in this region. Innervation of basal dendrites by mossy fiber axons creates functional recurrent circuits within the dentate (Ribak et al., 2000; Austin and Buckmaster, 2004; Shapiro and Ribak, 2006; Thind et al., 2008), potentially promoting hyperexcitability (Morgan and Soltesz, 2008). Finally, hilar mossy cells are commonly lost after epileptogenic brain injury. Mossy cells are glutamatergic excitatory neurons located in the dentate hilus that mediate both monosynaptic recurrent excitation and polysynaptic (via inhibitory GABAergic basket cells) recurrent inhibition of DGCs (Scharfman, 1995; Jackson and Scharfman, 1996; Ribak and Shapiro, 2007; Scharfman and Myers, 2012). Loss of these neurons is hypothesized to contribute to epileptogenesis by upsetting the balance of excitation and inhibition (Sloviter et al., 2012).

A key finding of the present study is that no single DGC pathology was able to account for seizure frequency in all animals. Rather, our data suggest that, to varying degrees, all four contribute. Even basal dendrites, which did not produce a significant correlation, still exhibited notable trends. However, correlation does not prove causation, and one interpretation of these findings is that some (or all) reflect epiphenomena. Perhaps some feature yet to be examined will fully account for epileptogenesis, or only one of the changes examined here is truly epileptogenic, with the others occurring as secondary consequences of the first. Consistent with this latter idea, MFS may be a consequence of mossy cell loss rather than a cause of epilepsy (Buckmaster, 2012). Mossy cells innervate the portion of DGC apical dendrites located within the IML. Extensive loss of mossy cells in rodent SE models of epilepsy partially deafferents these dendritic segments, creating an opportunity for innervation by sprouted DGC axons. Accordingly, MFS has been shown to directly correlate to mossy cell loss after pilocarpine-induced SE (Jiao and Nadler, 2007; but see also Volz et al., 2011; Jinde et al., 2012). A similar correlation was found in the present study.

It is also possible that multiple pathological changes act in concert to produce the epileptic state, potentially with different patterns of change accounting for the seizure phenotype in each animal. To explore this idea, we tabulated the data for all the animals (Table 2) and queried whether differences among the four parameters—either alone or in combination—could account for the biggest differences in seizure frequency. Interestingly, we found that, although no single variable increased from animal to animal as seizure frequency increased, in almost all cases at least one of the four variables increased. Although speculative, these findings are consistent with the idea that seizure frequency in each animal reflects the combined effects of multiple pathological changes and that these changes can pool in many different ways to produce the seizure phenotype for the animal.

References

Ahn S, Joyner AL (2004) Dynamic changes in the response of cells to positive hedgehog signaling during mouse limb patterning. Cell 118:505–516. CrossRef Medline

Ahn S, Joyner AL (2005) In vivo analysis of quiescent adult neural stem cells responding to Sonic hedgehog. Nature 437:894–897. CrossRef Medline

Austin JE, Buckmaster PS (2004) Recurrent excitation of granule cells with basal dendrites and low interneuron density and inhibitory postsynaptic current frequency in the dentate gyrus of macaque monkeys. J Comp Neurol 476:205–218. CrossRef Medline

Bajorat R, Wilde M, Sellmann T, Kirschstein T, Köhling R (2011) Seizure frequency in pilocarpine-treated rats is independent of circadian rhythm. Epilepsia 52:e118–e122. CrossRef Medline

Bonde S, Ekdahl CT, Lindvall O (2006) Long-term neuronal replacement in adult rat hippocampus after status epilepticus despite chronic inflammation. Eur J Neurosci 23:965–974. CrossRef Medline

Buckmaster PS (2012) Mossy fiber sprouting in the dentate gyrus. In: Jasper's basic mechanisms of the epilepsies, Ed 4. Bethesda, MD: National Center for Biotechnology Information.

Buckmaster PS, Dudek FE (1999) In vivo intracellular analysis of granule cell axon reorganization in epileptic rats. J Neurophysiol 81:712–721. Medline

Cameron MC, Zhan RZ, Nadler JV (2011) Morphologic integration of hilar ectopic granule cells into dentate gyrus circuitry in the pilocarpine model of temporal lobe epilepsy. J Comp Neurol 519:2175–2192. CrossRef Medline

Castro OW, Santos VR, Pun RY, McKlveen JM, Batie M, Holland KD, Gardner M, Garcia-Cairasco N, Herman JP, Danzer SC (2012) Impact of corticosterone treatment on spontaneous seizure frequency and epileptiform activity in mice with chronic epilepsy. PLoS One 7:e46044. CrossRef Medline

Cronin J, Dudek FE (1988) Chronic seizures and collateral sprouting of

dentate mossy fibers after kainic acid treatment in rats. Brain Res 474: 181–184. CrossRef Medline

Danzer SC (2012) Depression, stress, epilepsy and adult neurogenesis. Exp Neurol 233:22–32. CrossRef Medline

Danzer SC, He X, Loepke AW, McNamara JO (2010) Structural plasticity of dentate granule cell mossy fibers during the development of limbic epilepsy. Hippocampus 20:113–124. CrossRef Medline

Dashtipour K, Tran PH, Okazaki MM, Nadler JV, Ribak CE (2001) Ultrastructural features and synaptic connections of hilar ectopic granule cells in the rat dentate gyrus are different from those of granule cells in the granule cell layer. Brain Res 890:261–271. CrossRef Medline

de Lanerolle NC, Lee TS, Spencer DD (2012) Histopathology of human epilepsy. In: Jasper's basic mechanisms of the epilepsies (Noebels JL, Avoli M, Rogawski MA, Olsen RW, Delgado-Escueta AV, eds), Ed 4. Bethesda, MD: National Center for Biotechnology Information.

Fanselow MS, Dong HW (2010) Are the dorsal and ventral hippocampus functionally distinct structures? Neuron 65:7–19. CrossRef Medline

Fournier NM, Andersen DR, Botterill JJ, Sterner EY, Lussier AL, Caruncho HJ, Kalynchuk LE (2010) The effect of amygdala kindling on hippocampal neurogenesis coincides with decreased reelin and DISC1 expression in the adult dentate gyrus. Hippocampus 20:659–671. CrossRef Medline

Fujise N, Kosaka T (1999) Mossy cells in the mouse dentate gyrus: identification in the dorsal hilus and their distribution along the dorsoventral axis. Brain Res 816:500–511. CrossRef Medline

Goffin K, Nissinen J, Van Laere K, Pitkänen A (2007) Cyclicity of spontaneous recurrent seizures in pilocarpine model of temporal lobe epilepsy in rat. Exp Neurol 205:501–505. CrossRef Medline

Golarai G, Sutula TP (1996) Functional alterations in the dentate gyrus after induction of long-term potentiation, kindling, and mossy fiber sprouting. J Neurophysiol 75:343–353. Medline

Gorter JA, van Vliet EA, Aronica E, Lopes da Silva FH (2001) Progression of spontaneous seizures after status epilepticus is associated with mossy fibre sprouting and extensive bilateral loss of hilar parvalbumin and somatostatin-immunoreactive neurons. Eur J Neurosci 13:657–669. CrossRef Medline

Han Y, Spassky N, Romaguera-Ros M, Garcia-Verdugo J, Aguilar A, Schneider-Maunoury S, Alvarez-Buylla A (2008) Hedgehog signaling and primary cilia are required for the formation of adult neural stem cells. Nat Neurosci 11:277–284. CrossRef Medline

Haut SR, Swick C, Freeman K, Spencer S (2002) Seizure clustering during epilepsy monitoring. Epilepsia 43:711–715. CrossRef Medline

Haut SR, Lipton RB, LeValley AJ, Hall CB, Shinnar S (2005) Identifying seizure clusters in patients with epilepsy. Neurology 65:1313–1315. CrossRef Medline

Howell K, Hopkins N, Mcloughlin P (2002) Combined confocal microscopy and stereology: a highly efficient and unbiased approach to quantitative structural measurement in tissues. Exp Physiol 87:747–756. Medline

Jackson MB, Scharfman HE (1996) Positive feedback from hilar mossy cells to granule cells in the dentate gyrus revealed by voltage-sensitive dye and microelectrode recording. J Neurophysiol 76:601–616. Medline

Jessberger S, Zhao C, Toni N, Clemenson GD Jr, Li Y, Gage FH (2007) Seizure-associated, aberrant neurogenesis in adult rats characterized with retrovirus-mediated cell labeling. J Neurosci 27:9400–9407. CrossRef Medline

Jiao Y, Nadler JV (2007) Stereological analysis of GluR2-immunoreactive hilar neurons in the pilocarpine model of temporal lobe epilepsy: correlation of cell loss with mossy fiber sprouting. Exp Neurol 205:569–582. CrossRef Medline

Jinde S, Zsiros V, Jiang Z, Nakao K, Pickel J, Kohno K, Belforte JE, Nakazawa K (2012) Hilar mossy cell degeneration causes transient dentate granule cell hyperexcitability and impaired pattern separation. Neuron 76:1189–1200.

Jinno S (2011) Topographic differences in adult neurogenesis in the mouse hippocampus: a stereology-based study using endogenous markers. Hippocampus 21:467–480. CrossRef Medline

Jung KH, Chu K, Kim M, Jeong SW, Song YM, Lee ST, Kim JY, Lee SK, Roh JK (2004) Continuous cytosine-β-D-arabinofuranoside infusion reduces ectopic granule cells in adult rat hippocampus with attenuation of spontaneous recurrent seizures following pilocarpine-induced status epilepticus. Eur J Neurosci 19:3219–3226. CrossRef Medline

Jung KH, Chu K, Lee ST, Kim J, Sinn DI, Kim JM, Park DK, Lee JJ, Kim SU, Kim M, Lee SK, Roh JK (2006) Cyclooxygenase-2 inhibitor, celecoxib, inhibits the altered hippocampal neurogenesis with attenuation of spontaneous recurrent seizures following pilocarpine-induced status epilepticus. Neurobiol Dis 23:237–246. CrossRef Medline

Kaplan MS, Hinds JW (1977) Neurogenesis in the adult rat: electron microscopic analysis of light radioautographs. Science 197:1092–1094. CrossRef Medline

Kron MM, Zhang H, Parent JM (2010) The developmental stage of dentate granule cells dictates their contribution to seizure-induced plasticity. J Neurosci 30:2051–2059. CrossRef Medline

Kuruba R, Hattiangady B, Shetty AK (2009) Hippocampal neurogenesis and neural stem cells in temporal lobe epilepsy. Epilepsy Behav 14 [Suppl 1]:65–73. CrossRef

Lai K, Kaspar BK, Gage FH, Schaffer DV (2003) Sonic hedgehog regulates adult neural progenitor proliferation in vitro and in vivo. Nat Neurosci 6:21–27. CrossRef Medline

Lien EA, Solheim E, Ueland PM (1991) Distribution of tamoxifen and its metabolites in rat and human tissues during steady-state treatment. Cancer Res 51:4837–4844. Medline

Mathern GW, Bertram EH 3rd, Babb TL, Pretorius JK, Kuhlman PA, Spradlin S, Mendoza D (1997) In contrast to kindled seizures, the frequency of spontaneous epilepsy in the limbic status model correlates with greater aberrant fascia dentata excitatory and inhibitory axon sprouting, and increased staining for *N*-methyl-D-aspartate, AMPA and GABA(A) receptors. Neuroscience 77:1003–1019. CrossRef Medline

McAuliffe JJ, Bronson SL, Hester MS, Murphy BL, Dahlquist-Topal á R, Richards DA, Danzer SC (2011) Altered patterning of dentate granule cell mossy fiber inputs onto CA3 pyramidal cells in limbic epilepsy. Hippocampus 21:93–107. CrossRef Medline

McCloskey DP, Hintz TM, Pierce JP, Scharfman HE (2006) Stereological methods reveal the robust size and stability of ectopic hilar granule cells after pilocarpine-induced status epilepticus in the adult rat. Eur J Neurosci 24:2203–2210. CrossRef Medline

Morgan RJ, Soltesz I (2008) Nonrandom connectivity of the epileptic dentate gyrus predicts a major role for neuronal hubs in seizures. Proc Natl Acad Sci U S A 105:6179–6184. CrossRef Medline

Murphy BL, Pun RY, Yin H, Faulkner CR, Loepke AW, Danzer SC (2011) Heterogeneous integration of adult-generated granule cells into the epileptic brain. J Neurosci 31:105–117. CrossRef Medline

Murphy BL, Hofacer RD, Faulkner CN, Loepke AW, Danzer SC (2012) Abnormalities of granule cell dendritic structure are a prominent feature of the intrahippocampal kainic acid model of epilepsy despite reduced postinjury neurogenesis. Epilepsia 53:908–921. CrossRef Medline

Nadler JV (2003) The recurrent mossy fiber pathway of the epileptic brain. Neurochem Res 28:1649–1658. CrossRef Medline

Nakamura T, Colbert MC, Robbins J (2006) Neural crest cells retain multipotential characteristics in the developing valves and label the cardiac conduction system. Circ Res 98:1547–1554. CrossRef Medline

Nissinen J, Lukasiuk K, Pitkänen A (2001) Is mossy fiber sprouting present at the time of the first spontaneous seizures in rat experimental temporal lobe epilepsy? Hippocampus 11:299–310. CrossRef Medline

Parent JM, Lowenstein DH (2002) Seizure-induced neurogenesis: are more new neurons good for an adult brain? Prog Brain Res 135:121–131. CrossRef Medline

Parent JM, Yu TW, Leibowitz RT, Geschwind DH, Sloviter RS, Lowenstein DH (1997) Dentate granule cell neurogenesis is increased by seizures and contributes to aberrant network reorganization in the adult rat hippocampus. J Neurosci 17:3727–3738. Medline

Parent JM, Elliott RC, Pleasure SJ, Barbaro NM, Lowenstein DH (2006) Aberrant seizure-induced neurogenesis in experimental temporal lobe epilepsy. Ann Neurol 59:81–91. CrossRef Medline

Paxinos G, Franklin KB (2001) The mouse brain in stereotaxic coordinates. London: Academic.

Pitkanen A, Nissinen J, Lukasiuk K, Jutila L, Paljarvi L, Salmenpera T, Karkola K, Vapalahti M, Ylinen A (2000) Association between the density of mossy fiber sprouting and seizure frequency in experimental and human temporal lobe epilepsy. Epilepsia 41 [Suppl 6]:S24–S29.

Pozniak CD, Pleasure SJ (2006) A tale of two signals: Wnt and Hedgehog in dentate neurogenesis. Sci STKE 319:pe5. CrossRef Medline

Pun RY, Rolle IJ, Lasarge CL, Hosford BE, Rosen JM, Uhl JD, Schmeltzer SN, Faulkner C, Bronson SL, Murphy BL, Richards DA, Holland KD, Danzer SC (2012) Excessive activation of mTOR in postnatally generated gran-

ule cells is sufficient to cause epilepsy. Neuron 75:1022–1034. CrossRef Medline

Racine RJ (1972) Modification of seizure activity by electrical stimulation. II. Motor seizure. Electroencephalogr Clin Neurophysiol 32:281–294. CrossRef Medline

Ribak CE, Shapiro LA (2007) Ultrastructure and synaptic connectivity of cell types in the adult rat dentate gyrus. Prog Brain Res 163:155–166. CrossRef Medline

Ribak CE, Tran PH, Spigelman I, Okazaki MM, Nadler JV (2000) Status epilepticus-induced hilar basal dendrites on rodent granule cells contribute to recurrent excitatory circuitry. J Comp Neurol 428:240–253. CrossRef Medline

Ribak CE, Shapiro LA, Yan XX, Dashtipour K, Nadler JV, Obenaus A, Spigelman I, Buckmaster PS (2012) Seizure-induced formation of basal dendrites on granule cells of the rodent dentate gyrus. In: Jasper's basic mechanisms of the epilepsies, Ed 4. Bethesda, MD: National Center for Biotechnology Information.

Sanchez RM, Ribak CE, Shapiro LA (2012) Synaptic connections of hilar basal dendrites of dentate granule cells in a neonatal hypoxia model of epilepsy. Epilepsia 53 [Suppl 1]:98–108. CrossRef

Santos VR, de Castro OW, Pun RY, Hester MS, Murphy BL, Loepke AW, Garcia-Cairasco N, Danzer SC (2011) Contributions of mature granule cells to structural plasticity in temporal lobe epilepsy. Neuroscience 197:348–357. CrossRef Medline

Scharfman HE (1995) Electrophysiological evidence that dentate hilar mossy cells are excitatory and innervate both granule cells and interneurons. J Neurophysiol 74:179–194. Medline

Scharfman HE, Myers CE (2012) Hilar mossy cells of the dentate gyrus: a historical perspective. Front Neural Circuits 6:106. CrossRef Medline

Scharfman HE, Pierce JP (2012) New insights into the role of hilar ectopic granule cells in the dentate gyrus based on quantitative anatomic analysis and three-dimensional reconstruction. Epilepsia 53 [Suppl 1]:109–115. CrossRef

Scharfman HE, Goodman JH, Sollas AL (2000) Granule-like neurons at the hilar/CA3 border after status epilepticus and their synchrony with area CA3 pyramidal cells: functional implications of seizure-induced neurogenesis. J Neurosci 20:6144–6158. Medline

Scharfman HE, Smith KL, Goodman JH, Sollas AL (2001) Survival of dentate hilar mossy cells after pilocarpine-induced seizures and their synchronized burst discharges with area CA3 pyramidal cells. Neuroscience 104:741–759. CrossRef Medline

Shapiro LA, Ribak CE (2006) Newly born dentate granule neurons after pilocarpine-induced epilepsy have hilar basal dendrites with immature synapses. Epilepsy Res 69:53–66. CrossRef Medline

Sloviter RS (1987) Decreased hippocampal inhibition and a selective loss of interneurons in experimental epilepsy. Science 235:73–76. CrossRef Medline

Sloviter RS, Bumanglag AV, Schwarcz R, Frotscher M (2012) Abnormal dentate gyrus network circuitry in temporal lobe epilepsy. In: Jasper's basic mechanisms of the epilepsies, Ed 4. Bethesda, MD: National Center for Biotechnology Information.

Spigelman I, Yan XX, Obenaus A, Lee EY, Wasterlain CG, Ribak CE (1998) Dentate granule cells form novel basal dendrites in a rat model of temporal lobe epilepsy. Neuroscience 86:109–120. CrossRef Medline

Sutula TP, Dudek FE (2007) Unmasking recurrent excitation generated by mossy fiber sprouting in the epileptic dentate gyrus: an emergent property of a complex system. Prog Brain Res 163:541–563. CrossRef Medline

Tauck DL, Nadler JV (1985) Evidence of functional mossy fiber sprouting in hippocampal formation of kainic acid-treated rats. J Neurosci 5:1016–1022. Medline

Thind KK, Ribak CE, Buckmaster PS (2008) Synaptic input to dentate granule cell basal dendrites in a rat model of temporal lobe epilepsy. J Comp Neurol 509:190–202. CrossRef Medline

Volz F, Bock HH, Gierthmuehlen M, Zentner J, Haas CA, Freiman TM (2011) Stereologic estimation of hippocampal GluR2/3- and calretinin-immunoreactive hilar neurons (presumptive mossy cells) in two mouse models of temporal lobe epilepsy. Epilepsia 52:1579–1589. CrossRef Medline

Walter C, Murphy BL, Pun RY, Spieles-Engemann AL, Danzer SC (2007) Pilocarpine-induced seizures cause selective time-dependent changes to adult-generated hippocampal dentate granule cells. J Neurosci 27:7541–7552. CrossRef Medline